Preliminary Study on the Cloud Condensation Nuclei (CCN) Activation of Soot Particles by a Laboratory-scale Model Experiments

Chang-Jin Ma* and Ki-Hyun Kim[1)]

Department of Environmental Science, Fukuoka Women's University, Fukuoka 813-8529, Japan
[1)]Department of Civil & Environmental Engineering, Hanyang University, Seoul 133-791, Korea

*Corresponding author. Tel: +81-92-661-2411, E-mail: ma@fwu.ac.jp

ABSTRACT

To visually and chemically verify the rainout of soot particles, a model experiment was carried out with the cylindrical chamber (0.2 m (D) and 4 m (H)) installing a cloud drop generator, a hydrotherometer, a particle counter, a drop collector, a diffusing drier, and an artificial soot particle distributer. The processes of the model experiment were as follows; generating artificial cloud droplets (major drop size : 12-14 µm) until supersaturation reach at 0.52%-nebulizing of soot particles (JIS Z 8901) with an average size of 0.5 µm-counting cloud condensation nuclei (CCN) particles and droplets by OPC and the fixation method (Ma *et al.*, 2011; Carter and Hasegawa, 1975), respectively - collecting of individual cloud drops - observation of individual cloud drops by SEM - chemical identifying of residual particle in each individual droplet by SEM-EDX. After 10 minutes of the completion of soot particle inject, the number concentrations of PM of all sizes (>0.3 µm) dramatically decreased. The time required to return to the initial conditions, i.e., the time needed to CCN activation for the fed soot particles was about 40 minutes for the PM sized from 0.3-2.0 µm. The EDX spectra of residual particles left at the center of individual droplet after evaporation suggest that the soot particles seeded into our experimental chamber obviously acted as CCN. The coexistence of soot and mineral particle in single droplet was probably due to the coalescence of droplets (i.e., two droplets embodying different particles (in here, soot and background mineral particles) were coalesced) or the particle capture by a droplet in our CCN chamber.

Key words: Cloud condensation nuclei (CCN), Rain out, Black carbon, Soot particle, Cloud droplet, Chamber experiment

1. INTRODUCTION

The increasing energy consumption in the past century has led to ever greater emissions of elemental carbon (EC) or black carbon (BC) into atmosphere. BC is a major component of "soot" formed by the incomplete combustion of various fuels like fossil fuel and biomass (Ghan and Penner, 1992; Medalia *et al.*, 1983).

The lifetime of soot particles in the atmosphere is about seven days. During residence in the atmosphere, they contribute to the adverse impacts on human health and ecosystems associated with fine particulate matter (PM). Most of soot particles (about 98%) suspended in the air are finally removed by precipitation scavenging mechanisms (Jacobson, 2004).

BC is the most strongly light-absorbing component of PM. It can absorb million times more energy than carbon dioxide (CO_2) (U.S. EPA U.S., 2012). Thus, its increase in the atmosphere may affect the solar radiation balance and finally causes changes in radiative heating of the atmosphere and surface and the reduction of visibility.

Although fresh BC is mostly hydrophobic, the aged BC is most often found to be coated with water soluble compounds such as sulfate and organic carbon (Posfai *et al.*, 1999; Weingarther *et al.*, 1997). Once BC is aged (i.e., becoming sufficiently hydrophilic), then they can act as cloud condensation nuclei (CCN) (i.e., act as nuclei for CCN) in a supersaturated environment. This nucleation scavenging (i.e., rainout) is one of the most important processes governing the atmospheric lifetime of BC including other PM. BC that is activated as CCN will have shorter atmospheric lifetimes than that unaffected by nucleation. Furthermore, the nucleation properties of BC influence cloud microphysical and radiative properties, and consequently aerosol indirect radiative forcing (IPCC, 2007).

The CCN activation by water-soluble aerosols such as sulfates (O'Dowd *et al.*, 1999) and an inorganic salt

mixed with a single organic substance (Burkart *et al.*, 2011) are well documented. Till now, many field studies on the CCN activation of carbonaceous materials have been carried out (Cubison *et al.*, 2008; Broekhuizen *et al.*, 2006; Hitzenberger *et al.*, 1999).

However, much less experimental studies on CCN activation of carbonaceous PM have been done (Dusek *et al.*, 2006). Therefore, there is limited data available with respect to water vapor nucleation on carbonaceous particles.

The solar radiation absorbing properties of the cloud droplets formed by BC are influenced by the location of soot aerosol activated as CCN in droplet. If BC is located near the edge of the droplet, the heating can be more enhanced than when soot is embedded in the center of cloud droplets (Chýlek *et al.*, 1996). This indicates that the positional information of soot particle activated as CCN in a droplet has far greater value

than the simple confirm of CCN activation of soot particle.

In this study, for the purpose of experimental verification of the CCN activation of soot particles, a laboratory-scale model experiment was carried out. Moreover, an attempt was made to visually and chemically demonstrate the soot particles acted as CCN activation.

2. EXPERIMENTAL METHODS

2.1 Description of the Experimental Setup

For the experimental verification of the rainout of soot particles, a laboratory-scale experimental setup was designed. It consists of a small chamber (D 0.2 m, H 4.0 m), an artificial soot particle distributer, a drop generator, a hydrotherometer, a diffusion dryer, and an optical particle counter (Fig. 1, a: CCN chamber
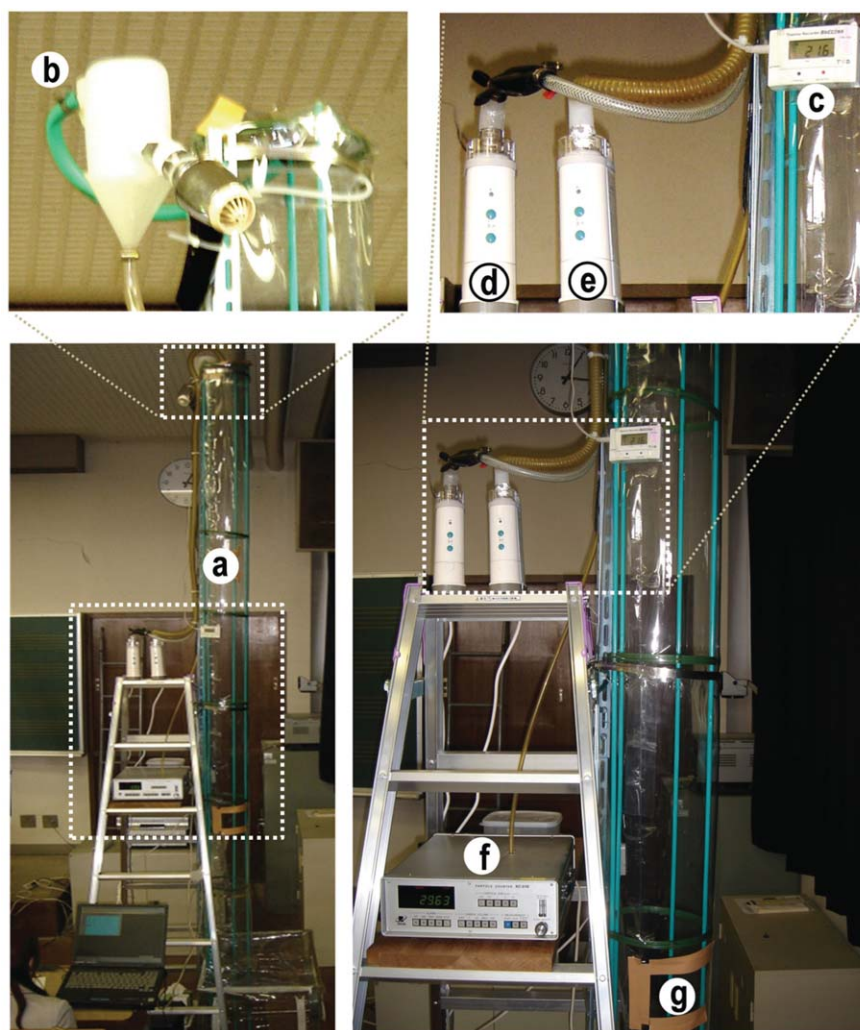

Fig. 1. Experimental set up to study the rainout of soot particles.
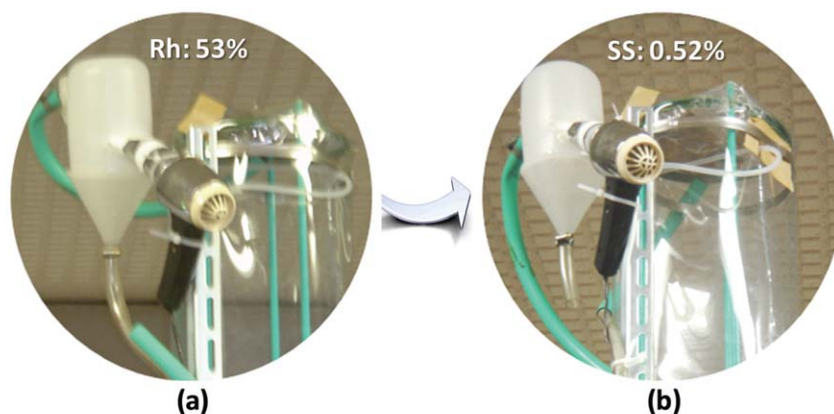
Fig. 2. Inner views of experimental chamber before (a) and after (b) droplet nebulizing.

(inlab-made), b: agitator with a dryer (hand-made), c: hydrothermal meter (S.S. Inc., TR-72U), d: nebulizer I (Omron Co., NE-U07), e: nebulizer II (Omron Co., NE-U07), f: OPC (RION Co., KC-01D1), and g: drop collector entrance)). Our experimental setup was located in the lab close to a window.

2.2 Procedures of a Laboratorial Model Experiment

The procedures adopted in this study for the laboratory-scale experiment were as follows:

(1) In this study, our CCN chamber was not refilled with the particle free dry air. A benefit of the soot particle seeding into our CCN chamber containing background particles is to demonstrate the coalescence of droplets activated from chemically different particles types (i.e., soot and other background mineral particles). In the static mode (i.e., stable initial mode), the background PM in our CCN chamber (Period I, initial condition in Fig. 5), the number concentrations of size-classified PM were 25700, 1750, 225, 36, 7 L^{-1}, at size range of 0.3-0.5 µm, 0.5-1.0 µm, 1.0-2.0 µm, 2.0-5.0 µm, and >0.5 µm, respectively.

(2) The droplets were nebulized with ultra-pure water (18.2 MΩ) using Nebulizer I and then were fed into the CCN chamber until the inner chamber reached 0.52% supersaturation (Period II, Droplet inject (10 min.) in Fig. 5). The total number of injected droplets was roughly 6.7×10^6. However, the number of droplets distributed in our experimental chamber would be partially decreased due to initial droplet evaporation, droplet adherence to the inner surface of chamber, droplet coalescence, and gravitational settling. Fig. 2 shows the inner views of experimental chamber before and after droplet nebulizing.

(3) The artificial soot particles were employed as CCN particle in this study. The average size, density,
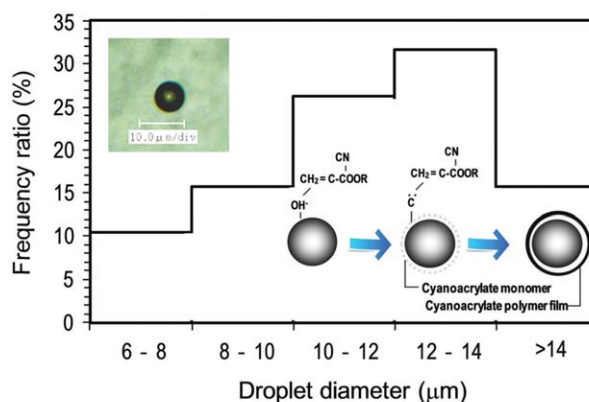

Fig. 3. Size distribution of droplets inflow into the experimental chamber.

and carbon content of the soot particles (JIS Z 8901) used in this study are 0.5 µm, 1.8 g cm^{-3}, and 98%, respectively (APPIE JIS Test Powders, 2004). These soot particles were diluted by high purity (99%) C_2H_5OH in a cup of nebulizer (lower left in Fig. 4). Since pure carbon is non-polar and hence will not dissolve in water (i.e., it is incapable of forming hydrogen bonds in water), it will only disperse in water as a colloidal solution rather than a true solution. Meanwhile, activated carbon is the world's best known medium for purification of alcohol (Gert Strand, 2001). Very low size droplets (approximately 5 µm diameter) (Austrian Standards Institute, 2010) containing soot particles were produced by the Nebulizer II employed in the present study. Then, the droplets passed through a diffusion dryer (Figs. 1 and 2) that removes C_2H_5OH from the soot particle-laden flow, and solid soot particles in air stream were injected into the top of CCN chamber. The total number of injected soot particles was approximately 9.5×10^7. It is roughly two times higher than
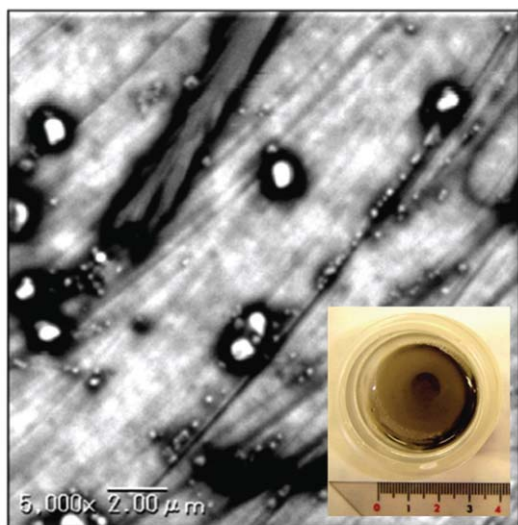
Fig. 4. An example of SEM image for soot particles on a Ag film installed at the outlet of drier ((b) in Fig. 1) and a cup of NebulizerII (lower left in Fig. 4) containing a 30 ml of C_2H_5OH including soot particles (JIS Z 8901 Test Powders).

the CCN number measured in the cloud of the summit of Mt. Fuji, Japan (Watanabe *et al.*, 2014). But this number is smaller than that (1.5×10^8) of the field study carried out by Hitzenberger *et al.* (1999) in spring, Vienna, Austria.

(4) The CCN and droplets concentrations were measured on a time scale of 1 min. In a measurement cycle, the CCN chamber was flushed for 30 minutes in interval of each experiment.

3. RESULTS AND DISCUSSION

3.1 Supersaturation Conditioning in a CCN Chamber

According to the Köhler theory (Köhler, 1936), the activation of CCN into cloud droplets depends on particle hygroscopicity, particle diameter, and water vapor supersaturation.

From field cloud measurements made at the summit of Mt. Fuji, Watanabe *et al.* (2014) reported that the liquid water content (LWC) was recorded as 0.048 g m^{-3} and supersaturation was 0.52% at that time. In light of this field measurement, the degree of supersaturation in our CCN chamber was adjusted to 0.52% in this study.

In order to estimate the water vapor supersaturation in our CCN chamber, the LWC of injected droplets was determined by the polymeric water absorbent film (PWAF) method (Ma *et al.*, 2003), which can collect the droplets without disappear and has the keeping

ability of absorbed droplets without evaporation in the stage of an impactor. After setup of PWAF on the impaction plate of an impactor sampler (Sibata Co., Code 8007-3), droplet collection was done. And then the mass of droplets were measured by an electric microbalance (Sartorius M5P-F) with the lowest detectable mass of 1 μg. Finally, LWC of droplets cloud be calculated from the information of droplet mass (g) and air amount (m^3). From the result of several preliminary experiments for the adjustment of 0.048 g m^{-3} of LWC (i.e., 0.52% supersaturation), the amount of high purity water nebulized into our CCN chamber was determined. Fig. 2 shows the inner views of experimental chamber at initial sate (Rh 53%) and after droplet nebulizing (SS 0.52%).

3.2 Size Distribution of Droplets

In order to measure the size distribution of droplets inflow into the experimental chamber, the fixation method (Ma *et al.*, 2011; Carter and Hasegawa, 1975) was applied. As schematically illustrated inner of Fig. 3, the fixation pathway can be divided into three stages: (1) reaction initiation due to exposure of the α-cyanoacrylate monomer vapor to the water droplet (unstable droplet), (2) reaction continuation through polymerization reactions between the α-cyanoacrylate monomers (incomplete fixation), and (3) reaction completion (stable fixed droplet). More details about this fixation technique were described in a previous publication (Carter and Hasegawa, 1975). Microscopic examination of the fixed droplets can estimate the actual size of spherical droplets.

As shown in Fig. 3 including a real fixed droplet (left upper), the variation of size distribution of droplets shows the monomodal distribution (major peak formed at 12-14 μm) forming a quite large on size scale of 6 μm to larger than 14 μm. According to Austrian Standards Institute (2010), our size distribution result is quite similar to the result of cascade impactor measurements for particle size by SolAero Ltd. and OMRON HEALTHCARE Co., Ltd.

3.3 Size of Aerosolized Soot Particles

The real size of soot particles fed into CCN chamber could be estimated by scanning electron microscopy (SEM, KYENCE, VE-7800). The aerosolized and dried soot particles were passively collected on the Ag film with a purity of 99.99 wt% or higher.

One of the primary advantages of size measuring of soot particles by a SEM is the subsequent component analysis of soot particles by an EDX analytical system. Also, it is possible to confirm whether the droplets exhausted from the outlet of drier are transformed to original soot particles or not. However, the soundness
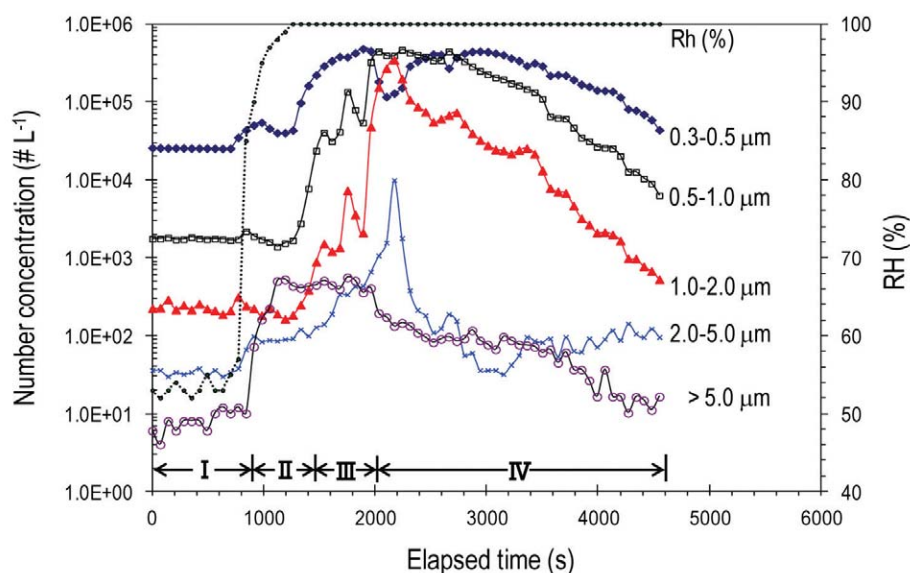
Fig. 5. Variation of particle number concentration during model experiment.

3. 4 Variation of Particle Number Concentrations during a Period of Model Experiment

of this method should be verified. The reliability of soot particle size measured by SEM observations was estimated by calculating the average size and their standard deviation of five different portions of an Ag film. A total of 100 soot particles randomly selected from each portion of Ag film was measured. The average size of soot particles for five different portions was 0.5 μm with a pretty low standard deviation (0.03 μm).

Fig. 4 shows a SEM image of soot particles on a Ag film installed at the outlet of drier ((b) in Fig. 1) and a cup of nebulizer II (lower left in Fig. 4) containing a 10 mL of C_2H_5OH including soot particles (JIS Z 8901 Test Powders). The size of the soot particles deposited on an Ag film was in the range 250 nm to 2.1 μm with an average 0.5 μm.

As stated above, PM nucleation properties, i.e., the characteristic of PM to form water droplets at atmospheric supersaturation levels, are determined by the particle size, chemical composition, and surface characteristics (Winkler, 1988; Köhler, 1936). In well-aged aerosol, the bulk of the BC mass is contained in particle sizes from 300 to 700 nm diameter (Kaneyasu and Murayama, 2000). Black carbon radiative heating effects on cloud microphysics should be the most significant in those CCNs that contain BC larger than a 500 nm diameter sphere (Conant et al., 2012). Therefore, it can be stated that the APPIE JIS Test Powders nebulized into the chamber have the ideal size to estimate of CCN activation.

Fig. 5 shows the variation of size-classified particle number concentration during a period of model experiment. In Fig. 5, I, II, III, and IV mean the periods of initial condition, droplet injection (10 min.), soot particle injection (10 min.), and CCN activation, respectively. This time serial particle number concentration severely fluctuated throughout the whole experimental period from I to IV. The number concentrations of size-resolved PM at four fractions (0.3-0.5 μm, 0.5-1.0 μm, 1.0-2.0 μm, and 2.0-5.0 μm) were seen to range from 433,018 to 480,640 L^{-1}, from 1,658 to 461,440 L^{-1}, from 184 to 343,812 L^{-1}, and from 90 to 9,848 L^{-1}, respectively.

In an earlier field studies made in winter and spring 1996 in Vienna, Austria (Hitzenberger et al., 1999), the CCN concentrations at 0.5% SS ranged from 500 cm^{-3} to 3,080 cm^{-3} in winter and ranged 170 cm^{-3} to 2,630 cm^{-3} in spring, respectively.

Although, all PM fractions do not act as CCN, the number concentration of PM of all sizes in this study is roughly similar to that of Hitzenberger et al.'s field study (Hitzenberger et al., 1999).

In general, the highly deliquescent particles, especially inorganic salts, exhibit pronounced deliquescence behavior in humid air. The growth of particles is influenced markedly not only by their chemical composition, but also by the initial particle size and ambient RH (Park et al., 2009). Thus, although some efforts
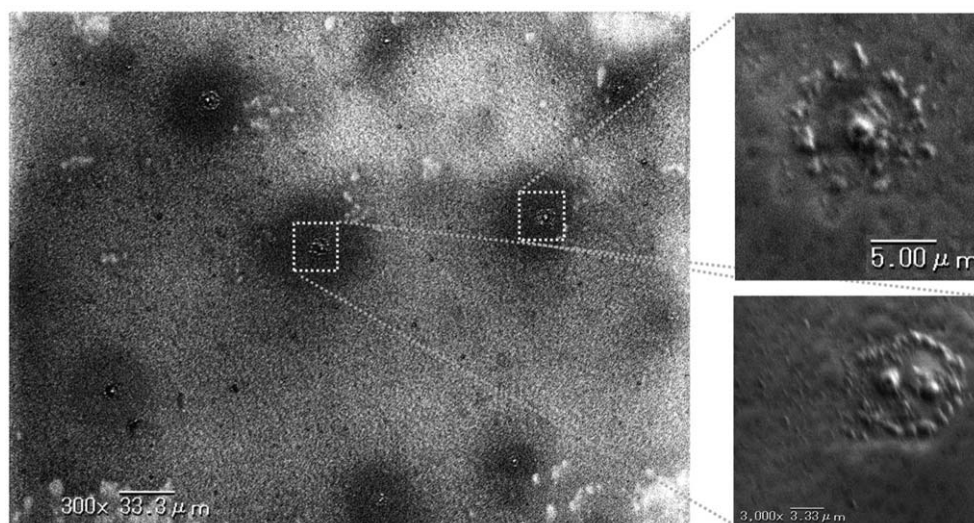
Fig. 6. The SEM images of the residual particles in dried droplets.

should be made to clearly affirm the growth of particles, the OPC data after droplet injection in Fig. 5 was probably influenced by the hygroscopic growth of some background particles.

Number concentrations of each size-sorted PM after soot particle injection increased 11, 278, 1,869, and 109 times at each PM size from 0.3 μm to 5.0 μm, respectively. Meanwhile, in the case of PM larger than 5 μm, a number concentration varied greatly from 9 to 501 L^{-1} during the period II, i.e., an inrush of droplet. After 10 minutes of the completion of soot particle inject, the number concentrations of PM of all sizes dramatically decreased. The time required to return to the initial condition was about 40 minutes for the PM sized from 0.3-2.0 μm. Large particles (2.0-5.0 μm), meanwhile, returned to the initial number concentration within only 10 minutes. This is probably due to the fact that larger particles can be more easily scavenged by cloud droplets (Stier *et al.*, 2006) and they were also gravitationally settled.

3.5 Residual Particles Embedded in Droplets and Their Chemical Identification

Droplets were passively collected on Ag film at the drop collector entrance of our experimental set up ((g) in Fig. 1). The evaporation of droplet means that liquid on the droplet surface changes its phase and mixes with the surrounding air. Therefore, the deposited droplets were promptly transferred into an aerosol free clean chamber and dried at room temperature. Fig. 6 shows an example of the visual observations of SEM images for the residual particles in the dried droplet. As shown in Fig. 6, single (right upper of Fig. 6) and dual parti-
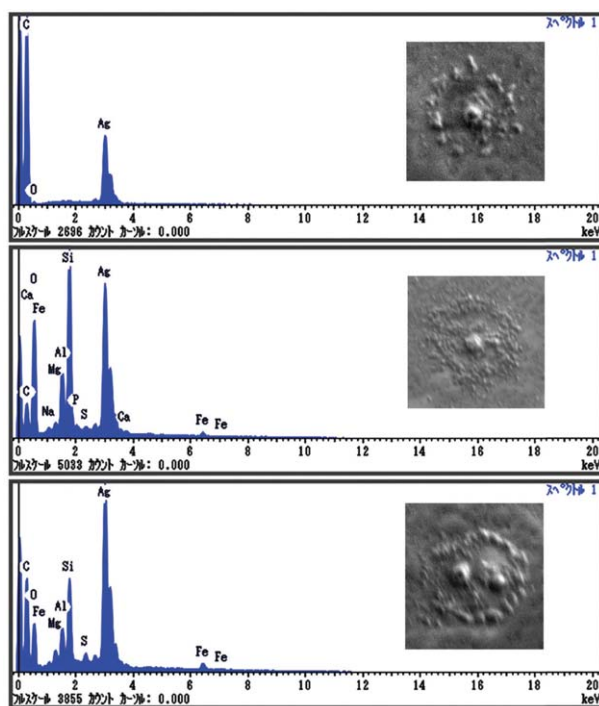

Fig. 7. The EDX spectra of residual particles left at the center of droplet after evaporation.

cles (right below of Fig. 6) were located at center of the dried droplet and they were surrounded by many dotted spots forming a ring.

When a droplet like a drop of coffee, tea, or water containing small solid particles is dried, it typically leaves a thin ring-shaped stain at droplet edges. This,
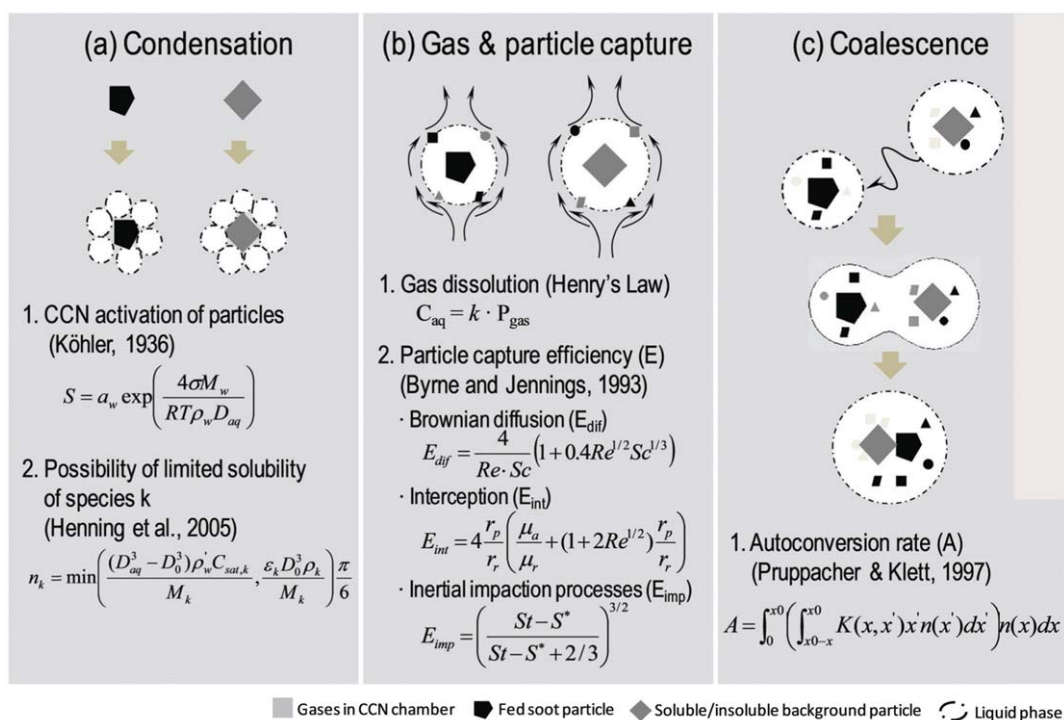
Fig. 8. A schematic to explain the expected cloud-microphysics process at each stage for condensation (left), gas and particle capture (middle), and coalescence (right).

known as the "coffee-ring" effect, is formed when the drop edges are pinned and subsequent radial capillary flows from the drop center to its edge carry suspended or dissolved solutes to the perimeter (Still *et al.*, 2012). In the case of the experiment employed aqueous suspensions of colloidal polystyrene particles with diameter $d=1330$ nm, nearly all particles were deposited in a thin ring and very few particles occupied the center of drop (Still *et al.*, 2012). At the present stage, we are unsure to conclude whether these particles placed at center of droplet are the soot particles (and/or background particles) fed into a CCN chamber. Consequently, in order to definitely investigate the chemical properties of the particles occupied the center of droplet, an electron probe of SEM-EDX (Swift ED 3000) was scanned on them. Fig. 7 shows the EDX spectra of residual particles left at the center of droplet after evaporation. At the top of Fig. 7, it was possible to resolve a unique C peak with Ag peak derived Ag film, whereas no meaningful peaks of other elements were detected. This spectrum property was very similar to that of the original soot particle (JIS Z 8901) nebulized into a CCN chamber. It thus suggests undoubtedly that the soot particles seeded into a CCN chamber acted as CCN, i.e., rainout mechanism should be capable of scavenging of soot particles in the ambient atmosphere. On the other hand, the mineral components (Si, Fe, Al,

and Mg) peaks were dominantly drawn at the middle of Fig. 7. It may well be the mineral particle existed as the background PM. Furthermore, the bottom of Fig. 7 is a most revealing EDX spectrum.

In order to understand the mechanisms of this elemental inhomogeneity in each cloud droplet, one has to consider three-step cloud-microphysics processes, i.e., condensation, gas and particle capture, and coalescence. The conceptional illustrations of cloud-microphysics processes are described in Fig. 8. The differences of elemental distribution in each individual cloud droplets arise from follows;

(1) Differences in the composition of the condensation nuclei (right side of Fig. 8)

(2) Different chemical components of the soluble gases (middle of Fig. 8)

(3) Various background particles transferred into droplets (middle of Fig. 8) by mainly three capturing processes (i.e., Brownian diffusion, direct-interception, and inertial impaction)

(4) Coalescence of droplets (i.e., the process by which two or more droplets or particles merge during contact to form a single daughter droplet) which contain different particles (right side of Fig. 8).

At the bottom of Fig. 7, the peak of C coexisting with those of several mineral components (i.e., Si, Al, Fe, and Mg) therefore suggests that these consolidated

elements in a droplet was probably due to the coalescence of droplets ((c) of Fig. 8) or the particle capture by a droplet ((b) of Fig. 8).

4. CONCLUSIONS

Although, the indirect climate effect of BC is widely understood, the rainout mechanisms of BC are still uncertain and CCN activation of BC is not yet visually demonstrated. In this study, for the purpose of experimental verification of the CCN activation of soot particles, a laboratory-scale model experiment was carried out. Moreover, an attempt was made to visually and chemically demonstrate the soot particles acted as CCN activation. The morphological preservation of CCN activation of BC was successfully made by the SEM observation of the residual particles in individual dried droplets. The EDX spectra of two residual particles left in a droplet suggest that droplet coalescence (or particle capture by a droplet) was also occurred in our CCN chamber. In 0.52% supersaturated situation of our CCN chamber, the injected soot particles began CCN activating in earnest after 10 minutes of the completion of soot particle injection. The time required to complete CCN activation for all fed soot particles (i.e., the time needed to return to the background particle number concentration) was about 30 minutes. Although, in our preliminary approach, the vast parameterization of CCN activation such as CCN/CN (condensation nucleus) cloud not be assessed satisfactorily, the unique outcomes of this study can verify the role of soot particles as CCN.

ACKNOWLEDGEMENT

REFERENCES

Activated carbon for purification of alcohol (2001) Internet publishing: Gert Strand, Malmoe, Sweden, pp. 1-28

APPIE JIS Test Powders (2004) The Association of Powder Process Industry and Engineering, Japan, pp. 1-4.

Austrian Standards Institute (2010) Respiratory therapy equipment, Part 1: Nebulizing systems and their components. Österreichisches Normungsinstitut (ON), Wien, pp. 1-43.

Broekhuizen, K., Chang, R.Y.W., Leaitch, W.R., Li, S.-M., Abbatt, J.P.D. (2006) Closure between measured and modeled cloud condensation nuclei (CCN) using size resolved aerosol compositions in downtown Toronto. Atmospheric Chemistry and Physics 6, 2513-2524.

Burkart, J., Steiner, G., Reischl, G., Hitzenberger, R. (2011) Long-term study of cloud condensation nuclei (CCN) activation of the atmospheric aerosol in Vienna. Atmospheric Environment 45, 5751-5759.

Byrne, M.A., Jennings, S.G. (1993) Scavenging of submicrometer aerosol-particles by water drop. Atmospheric Environment A 27, 2099-2105.

Carter, W.L., Hasegawa, I. (1975) Fixation of tobacco smoke aerosols for size distribution studies. Journal of Colloid Interface Science 53, 134-141.

Chýlek, P., Lesins, G., Videen, G., Wong, J., Pinnick, R., Ngo, D., Klett, J. (1996) Black carbon and absorption of solar radiation by clouds, Journal of Geophysical Research 101, 23365-23371.

Climate Change 2007, the Fourth Assessment Report (AR4) of the United Nations Intergovernmental Panel on Climate Change (IPCC).

Conant, W.C., Nenes, A., Seinfeld, J.H. (2012) Black carbon radiative heating effects on cloud microphysics and implications for the aerosol indirect effect 1. Extended Köhler theory. Journal of Geophysical Research: Atmospheres 107-D21, AAC 23-1-AAC 23-9.

Cubison, M.J., Ervens, B., Feingold, G., Docherty, K.S., Ulbrich, I.M., Shields, L., Prather, K., Hering, S., Jimenez, J.L. (2008) The influence of chemical composition and mixing state of Los Angeles urban aerosol on CCN number and cloud properties. Atmospheric Chemistry and Physics 8, 5649-5667.

Dusek, U., Reischl, G.P., Hitzenberger, R. (2006) CCN activation of pure and coated carbon black particles. Environmental Science and Technology 40, 1223-1230.

EPA of U.S. (2012) Basic Information, What is Black Carbon? http://www.epa.gov/black carbon/basic.html

Ghan, S.J., Penner, J.E. (1992) Smoke, effects on climate. Encyclopedia of Earth System Science 4, Academic Press, pp. 191-198.

Henning, S., Rosenorn, T., D'Anna, B., Gola, A.A., Svenningsson, B., Bilde, M. (2005) Cloud droplet activation and surface tension of mixtures of slightly soluble organics and inorganic salt. Atmospheric Chemistry and Physics 5, 575-582.

Hitzenberger, R., Berner, A., Giebl, H., Kromp, R., Larson, S.M., Rouc, A., Koch, A., Marischka, S., Puxbaum, H. (1999) Contribution of carbonaceous material to cloud condensation nuclei concentrations in European background (Mt. Sonnblick) and urban (Vienna) aerosols. Atmospheric Environment 33, 2647-2659.

Jacobson, M. (2004) Climate response on fossil fuel and biofuel soot, accounting for soot's feedback to snow and sea ice albedo and emissivity. Journal of Geophysical Research 109, 945, doi:10.1029/2004JD004.

Kaneyasu, N., Murayama, S. (2000) High concentrations

of black carbon over middle latitudes in the North Pacific Ocean. Journal of Geophysical Research 105, 19881-19890.

Köhler, H. (1936) The nucleus in the growth of hygroscopic droplets. Transactions of the Faraday Society 32, 1152-1161.

Ma, C.J., Kasahara, M., Tohno, S. (2003) Application of polymeric water absorbent film to the study of drop size-resolved fog samples. Atmospheric Environment 37, 3749-3756.

Ma, C.-J., Tohno, S., Kasahara, M. (2011) Preliminary study on visualization and quantification of the elemental compositions in individual micro droplet by the solidification and synchrotron radiation techniques. Asian Journal of Atmospheric Environment 5, 56-63.

Medalia, A., Rivin, D., Sanders, D. (1983) A comparison of carbon black with soot. Science of the Total Environment 31, 1-22.

O'Dowd, C.D, Lowe, J.A., Smith, M.H. (1999) Coupling sea-salt and sulphate interactions and its impact on cloud droplet concentration predictions. Geophysical Research Letter 26, 1311-1314.

Park, K., Kim, J.S., Miller, A.L. (2009). A Study on effects of size and structure on hygroscopicity of nanoparticles using a tandem differential mobility analyzer and TEM. Journal of Nanoparticle Research 11, 175-183.

Posfai, M., Anderson, J., Buseck, P., Sievering, H. (1999) Soot and sulfate aerosol particles in the remote marine troposphere, Journal of Geophysical Research 104, 21685-21693.

Pruppacher, H.R., Klett, J.D. (1997) Microphysics of clouds and precipitation, Kluwer Acad., Norwell, Mass. pp. 40-80.

Stier, P., Feichter, J., Roeckner, E., Kloster, S., Esch, M. (2006). Emission-induced nonlinearities in the global aerosol system. Journal of Climate 19, 3845-3862.

Still, T., Yunker, P.J., Yodh, A.G. (2012) Surfactant-induced Marangoni eddies alter the coffee-rings of evaporating colloidal drops. American Chemical Society 28, 4984-4988.

Varghese, S.K., Gangamma, S. (2007) Evaporation of water droplets by radiation: Effect of absorbing inclusions. Aerosol and Air Quality Research 7, 95-105.

Watanabe, S., Aoyagi, A., Miura, W., Furutani, K., Wuematsu, K., Ouhara, W. (2014) Concentration of CCN and cloud drop measured at the summit of Fuji Mt. 7th Report of the application of the base of Fuji Mt. pp. 34-35.

Weingartner, E., Burtscher, H., Baltensperger, U. (1997) Hygroscopic properties of carbon and diesel soot particles. Atmospheric Environment 31, 2311-2327.

Winkler, P. (1988) The growth of atmospheric aerosol particles with relative humidity. Physica Scripta 37, 223-230.